Journal of the Korean Society of Surveying, Geodesy, Photogrammetry and Cartography
Vol. 37, No. 5, 397-402, 2019
https://doi.org/10.7848/ksgpc.2019.37.5.397
ISSN 1598-4850(Print)
ISSN 2288-260X(Online)
Original article

Requirements Analysis of Image-Based Positioning Algorithm for Vehicles

Lee, Yong [1)] · Kwon, Jay Hyoun [2)]

Abstract

Recently, with the emergence of autonomous vehicles and the increasing interest in safety, a variety of research has been being actively conducted to precisely estimate the position of a vehicle by fusing sensors. Previously, researches were conducted to determine the location of moving objects using GNSS (Global Navigation Satellite Systems) and/or IMU (Inertial Measurement Unit). However, precise positioning of a moving vehicle has lately been performed by fusing data obtained from various sensors, such as LiDAR (Light Detection and Ranging), on-board vehicle sensors, and cameras. This study is designed to enhance kinematic vehicle positioning performance by using feature-based recognition. Therefore, an analysis of the required precision of the observations obtained from the images has carried out in this study. Velocity and attitude observations, which are assumed to be obtained from images, were generated by simulation. Various magnitudes of errors were added to the generated velocities and attitudes. By applying these observations to the positioning algorithm, the effects of the additional velocity and attitude information on positioning accuracy in GNSS signal blockages were analyzed based on Kalman filter. The results have shown that yaw information with a precision smaller than 0.5 degrees should be used to improve existing positioning algorithms by more than 10%.

Keywords : Vehicle Positioning System, Multi Sensor Integration, GNSS Signal Blockages, Kalman Filter

1. Introduction

It is very important to determine the precise position of a moving object to ensure the safety of the driver and pedestrians. In addition to the traditional integration of GNSS (Global Navigation Satellite System) with IMU (Inertial Measurement Unit), various research on using LiDAR (Light Detection and Ranging), cameras, and on-board vehicle sensors to the system have been actively conducted(Wei *et al*., 2018; Tsai *et al*., 2014). Recently, due to the development of computing technology, research is being carried out to generate additional observations from images acquired by cameras and to use them for positioning. Jung *et al*. (2017) performed SPR (Single Photo Resection) from three or more unique objects from images. It was used as an additional observation to improve positioning performance. However, SPR has a limitation that it is possible only when the absolute coordinates of the object of interest are known. In addition, Park *et al*. (2018) extracted the distance to an object of interest using stereo images, and calculated speed variation using image acquisition intervals. There is an advantage because the absolute coordinates are not necessary, but it is not possible to obtain the velocity if the object of interest is not in the image. One previous study was conducted to improve positional accuracy by extracting the velocity of the object. However, the feature of interest should be existed in

Received 2019. 10. 07, Revised 2019. 10. 23, Accepted 2019. 10. 25
1) Member, Dept. of Geoinformaticts, University of Seoul (E-mail: acce00@uos.ac.kr)
2) Corresponding Author, Member, Dept. of Geoinformatics, University of Seoul (E-mail : jkwon@uos.ac.kr)

the image to generate observations. Also, if the number of objects in the image is small, the positional accuracy could be degraded by error propagated from the observations. In order to overcome this problem, it is necessary to extract many feature points from an image and generate observations continuously, even if the object of interest is not in it. The limitations of an object-based recognition algorithm could be overcome by generating observations from arbitrary multiple feature points. A broad range of feature extraction algorithms have been developed in imaging field (Shi and Tomasi,1994; Harris, 1988). It is possible to extract the relative velocity and attitude information of a moving object from any feature point obtained by using a feature point extraction algorithm. Therefore, in this study, the required accuracy analysis of the velocity and attitude information from images is performed before implementing a feature-based image positioning algorithm. The effects of additional velocity and attitude information on a positioning algorithm using a GNSS, MEMS-IMU (Micro Electro-mechanical System–Inertial Measurement Unit), and magnetometer were analyzed. Assuming that the GNSS signal is disconnected for 30 seconds, a performance analysis was performed by calculating the two-dimensional positional error from the reference data.

2. Vehicle Positioning Algorithm

In this study, the effects of velocity and attitude information obtained from an image for the positioning accuracy of a vehicle were analyzed. Velocity and yaw information based on simulation is used to correct the navigation solution of a previously developed positioning algorithm. Among the vehicle positioning algorithms developed in the previous study (Lee and kwon, 2018), an IMU/GNSS/WSS (Wheel Speed Sensor) combination and an IMU/GNSS/WSS/MAG (Magnetometer) combination were used for analysis. The vehicle positioning algorithm basically calculates the position, attitude, and velocity of a moving object from the initial position by integrating the angular velocity and acceleration measured by the IMU. At this time, this compensates for navigation error if the velocity and position information obtained from a GNSS is available. If speed and attitude information is obtained from the wheel speed sensor or magnetometer, compensation for the navigation solution is conducted. Wheel speed sensors are used among the on-board vehicle sensors. The wheel speed sensor calculates the speed directly from the wheel of the vehicle. The average of both rear wheel speeds was taken to calculate the speed recorded by the wheel speed sensors (Han, 2016). All of the vehicle positioning algorithms were implemented using a weakly coupled Kalman filter, and the closed loop type was adopted to compensate for the estimated sensor error. The position and velocity obtained from the GNSS were obtained from the C/A (Course/Acquisition) code and Doppler observation, respectively. The GNSS update interval was 1 Hz. When acceleration and angular velocity are obtained from the IMU, the navigation equation is used to determine the attitude, velocity, and position at 100hz intervals from the initial position and attitude. Similarly, If speed is observed on both rear wheels, this is used to calculate the speed of the vehicle and to compensate for navigation solution at 1Hz. Observations obtained from the magnetometer are used to compensate the vehicle's yaw information, with an update interval of 1 Hz. Assuming that the velocity and attitude observations obtained from the images exist, navigational corrections were performed at intervals of 1 Hz. This is summarized in Fig. 1.

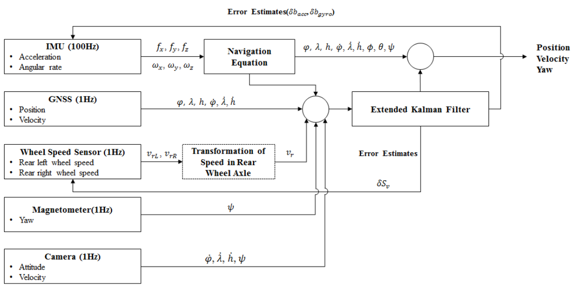

Fig. 1. A schematic diagram of the GNSS/MEMS-IMU/on-board vehicle sensor/magnetometer integration algorithm

3. Hardware Platform and Study Area

In this study, various sensors were mounted on vehicles to acquire data. The vehicle used in the experiment, shown in Fig. 2, was already equipped with an on-board vehicle sensor for ADAS(Advanced Driver Assistant System). In addition, the vehicle was equipped with a GNSS antenna, receiver, and MEMS-IMU. For the GNSS, the single-point positioning technique is applied to determine the position. According to specification of manufacture, the positional accuracy of a GNSS is known to be about 1.5 m using single point positioning. The magnetometer and MEMS-IMU (Xsens MTI-G-700) was used to acquire acceleration and angular velocity. The specifications of the accelerometer, gyroscope, and magnetometer are in Table 1. The specifications of the wheel speed sensor already installed in the vehicle are in Table 2. Reference data obtained from Applanix's POSLV turnkey position and orientation system enabled precise positioning. POSLV is known to have attitude and position errors of 0.015 deg and 2 cm, respectively.

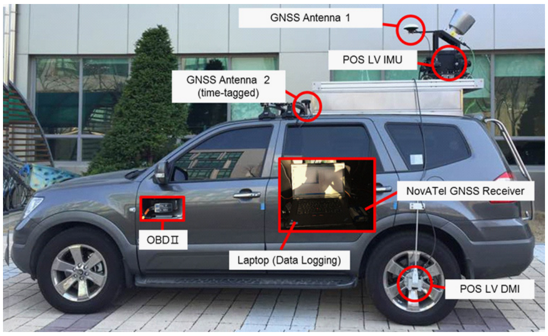

Fig. 2. Hardware platform of test vehicle (Han, 2016)

Table 1. Specifications of MEMS-IMU and magnetometer

	Output range	Bias repeatability	Noise density
Accelerometer	50 m/s²	40 μg	150 μg/√Hz/
Gyro scope	450 deg/s	0.5 deg/s	0.015 deg/s/√Hz
Magnetometer	+/- 80 μT	-	200 μG/√Hz

Table 2. Specifications wheel speed sensor

Output range	Resolution
0 ~ 511.75 km/h	0.125 km/h

Actual data for analysis were obtained by driving a car. The driving area was Daegu-Gyeongbuk Institute of Science and Technology and Technopolis. It took about 30 min for data acquisition, and the total range was about 11 km. For more detailed information on the data, see (Lee and Kwon, 2018). Velocity and attitude information assumed to have been acquired from the image was generated using reference data. We inferred the velocity information obtained from the image by adding random errors having standard deviations of 0.1 m/s, 0.5 m/s, and 1.0 m/s to the reference data. In the case of attitude, by adding random errors having standard deviations of 0.1 deg, 0.5 deg, and 1.0 deg to reference attitude, the error value added to the reference data was applied considering previous studies (Grimes and LeCun, 2009; Li *et al.*, 2019). GNSS signal disconnection situations were assumed for the performance analysis. In Fig. 3, the red lines indicate a signal disconnection for 30 seconds. A total of 10 sections of signal disconnection were intentionally generated.

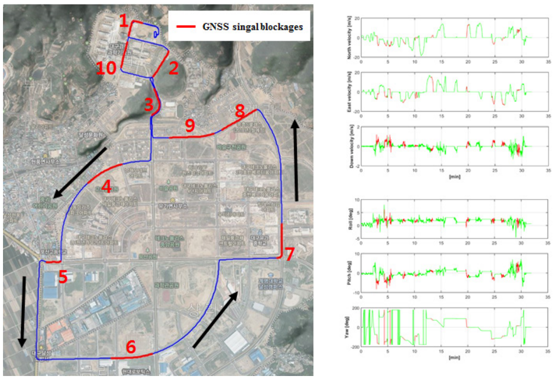

Fig. 3. Test Area, reference velocity and attitude

4. Results and Analysis

4.1 GNSS/IMU/WSS integration

Without velocity and yaw correction, the GNSS/IMU/WSS combination showed a two-dimensional position error of about 6.25 m on average during 10 GNSS signal outages. When the most accurate velocity and yaw corrections were performed, the average of the two-dimensional positioning errors was about 4.17 m during the 10 GNSS signal outages. The improvement rate was about 33.4%. Even when the velocity and yaw correction was performed with the magnitude of 1.0 error, the average of the two-dimensional position error was 4.54 m, which showed an improvement of 27.3% (Table 3). With the GNSS/IMU/

WSS combination, the effect of yaw correction was found to be effective. Since the wheel speed sensor only performs velocity correction, if yaw information is additionally obtained, and the navigation solution is corrected, we can see that the performance improvement is excellent during the GNSS signal disconnections. In particular, we can see that velocity and yaw correction is shown effectively in the first to third disconnection zones. The horizontal positional errors at GNSS outage zones 1 to 3 were reduced greatly. On the other hand, in the fourth and ninth sections, we can see that the two-dimensional position error is larger than the other sections.

As can be seen in Table 4, when the velocity and yaw correction is performed, the yaw error in GNSS signal outages 1, 2, and 3 were effectively removed. Sections 1, 2, and 3 are all sections that include a big change in direction. The yaw correction in the section containing the direction change showed improvement in positioning performance.

In the fourth and ninth sections, even if additional yaw information is obtained, the performance improvement was insignificant. Yaw information assumed to be acquired from the image did not significantly affect yaw correction.

4.2 GNSS/IMU/WSS/MAG Integration

The GNSS/IMU/WSS/MAG combination showed an average two-dimensional position error of about 3.79 m during 10 GNSS signal blockages without velocity and yaw compensation (Table 5). In the case of correction using the observation with the velocity and yaw errors of 1.0 magnitude, the mean of the two-dimensional error was 3.46 m, which showed a slight improvement of about 8.7% compared to making no corrections. Compared to the previous GNSS/IMU/WSS combination, the effect of velocity and yaw correction is smaller. In the GNSS/IMU/WSS/MAG combination, the yaw information obtained from the magnetometer was already corrected, and the effect is

Table 3. The horizontal error of GNSS/MEMS-IMU/WSS integration (unit : m)

Velocity error (m/s)	Yaw error (deg)	GNSS outage index										average (m)	Improvement (%)
		1	2	3	4	5	6	7	8	9	10		
0.1	0.1	0.32	0.31	0.08	18.99	1.80	3.61	0.31	2.67	12.74	0.82	4.17	33.4
	0.5	0.38	0.36	0.07	19.43	1.89	4.01	0.21	2.72	12.83	0.67	4.26	31.9
	1.0	1.23	1.64	0.61	19.50	1.95	4.30	0.15	2.73	12.85	0.56	4.55	27.2
0.5	0.1	0.54	1.12	0.42	18.69	1.79	3.67	0.25	2.63	12.65	0.77	4.25	31.9
	0.5	0.53	1.32	0.49	19.15	1.88	4.02	0.19	2.69	12.77	0.66	4.37	30.1
	1.0	0.86	1.56	0.59	19.55	1.95	4.29	0.15	2.73	12.86	0.56	4.51	27.8
1.0	0.1	0.68	1.18	0.46	18.67	1.79	3.67	0.25	2.63	12.64	0.77	4.27	31.6
	0.5	0.71	1.39	0.52	19.13	1.88	4.02	0.19	2.69	12.76	0.65	4.39	29.7
	1.0	1.09	1.65	0.63	19.53	1.95	4.30	0.15	2.73	12.86	0.56	4.54	27.3
Without correction		3.79	7.13	6.70	22.37	1.99	4.25	0.18	2.72	12.82	0.57	6.25	-

Table 4. The yaw error at the end of GNSS signal outages (unit: deg)

Velocity error (m/s)	Yaw error (deg)	GNSS outage index		
		1	2	3
0.1	0.1	-0.02	0.03	-0.01
0.5	0.5	-0.01	-0.03	-0.03
1.0	1.0	-0.04	-0.11	-0.06
without correction		2.23	-2.01	-2.67

smaller than the GNSS/IMU/WSS combination. In order to have a performance improvement of more than 10%, the accuracy of the yaw should be smaller than 0.5 deg. Outage 1 did not show significant improvement, unlike the previous GNSS/IMU/WSS combination. This is because yaw correction was already performed by the magnetometer. On the other hand, when low accuracy velocity information is added, the two-dimensional position error increases compared to the case without correction.

5. Summary and Conclusion

In this study, the required accuracy analysis was performed before implementing a feature-based image assistance algorithm. Velocity information and yaw information, which are assumed to be extracted from an image, were used for compensation in the navigation solution. For a performance analysis, GNSS signal disconnection was intentionally caused. Two-dimensional positional error with reference data was calculated under the GNSS signal disconnections.

In the GNSS/IMU/WSS combination, when observations with velocity and yaw accuracy of 1.0 m/s and 1.0 deg were used for compensation, the improvement rate was about 27.3%.

In the GNSS/MEMS-IMU/WSS/MAG combination, since yaw correction was already performed by the magnetometer, the effect of velocity and yaw correction was smaller than with the GNSS/IMU/WSS combination.

In order to expect an improvement of more than 10%, yaw information with accuracy of less than 0.5 deg should be applied for compensation.

In future research, we intend to calculate velocity and attitude from extracted feature points using actual images acquired from a camera. The results of this study are expected to be used as basic data for developing image-based positioning assistance algorithms using real images.

Acknowledgment

This work was supported by the 2019 sabbatical year research grant of the University of Seoul.

References

Grimes, M. and LeCun, Y. (2009), Efficient off-road localization using visually corrected odometry. *IEEE International Conference on Robotics and Automation*, 12-17 May, Kobe, Japan, pp. 2649-2654.

Han, J.H. (2016), Performance Analysis of Positioning through the Integration of GNSS and On-board Vehicle Sensors, Ph.D. dissertation, University of Seoul, Seoul, Korea, 162p.

Jung, J., Kwon, J.H., and Lee, Y. (2017), Development of Image-based Assistant Algorithm for Vehicle Positioning

Table 5. The horizontal error of GNSS/MEMS-IMU/WSS/MAG integration (unit: m)

Velocity error (m/s)	Yaw error (deg)	GNSS outage index										average (m)	Improvement (%)
		1	2	3	4	5	6	7	8	9	10		
0.1	0.1	0.19	0.06	0.34	12.31	0.08	1.13	5.92	1.62	5.01	4.17	3.08	18.8
	0.5	0.17	0.11	0.33	12.56	0.02	1.31	5.96	1.67	5.09	4.08	3.13	17.5
	1.0	0.07	0.15	0.31	12.74	0.02	1.45	5.99	1.70	5.14	4.01	3.16	16.8
0.5	0.1	1.25	0.28	0.54	12.27	0.06	1.19	5.99	1.53	4.95	4.23	3.23	15.0
	0.5	1.52	0.46	0.49	12.53	0.01	1.40	6.04	1.58	5.03	4.13	3.32	12.5
	1.0	2.03	0.65	0.40	12.74	0.06	1.56	6.08	1.62	5.09	4.05	3.43	9.7
1.0	0.1	1.49	0.29	0.57	12.26	0.05	1.19	5.99	1.52	4.94	4.23	3.25	14.2
	0.5	1.79	0.48	0.51	12.53	0.01	1.40	6.05	1.57	5.03	4.13	3.35	11.7
	1.0	2.34	0.68	0.42	12.74	0.06	1.57	6.08	1.61	5.09	4.05	3.46	8.7
Without correction		0.91	2.14	3.29	13.31	0.04	1.47	6.02	1.59	5.07	4.10	3.79	-

by Detecting Road Facilities. *Journal of the Korean Society of Surveying, Geodesy, Photogrammetry and Cartography*, Vol. 35, No. 5, pp. 339-347.

Lee, Y. and Kwon J.H. (2018), Performance analysis of the GNSS/MEMS-IMU/on-Board vehicle sensor/magnetometer-based positioning system during GNSS signal blockage, *International Journal of Urban Sciences* , Vol. 23, No. 3, pp. 1-10.

Li, T., Zhang, H., Gao, Z., Niu, X., and El-Sheimy, N. (2019), Tight Fusion of a Monocular Camera, MEMS-IMU, and Single-Frequency Multi-GNSS RTK for Precise Navigation in GNSS-Challenged Environments. *Remote Sensing*, Vol. 11, No. 6, pp. 1-24.

Park, J.S., Lee, Y., and Kwon, J.H. (2018), Performance Analysis of Vision-based Positioning Assistance Algorithm, Journal of the Korean Society of Surveying, *Geodesy, Photogrammetry and Cartography*, Vol. 37, No. 3, pp. 101-108. (in Korean with English abstract)

Tsai, F., Chang, H., and Su, A.Y.S. (2014), Combining MEMS-based IMU Data and Vision-based Trajectory Estimation, *The International Archives of the Photogrammetry, Remote Sensing and Spatial Information Sciences*, 14–16 May, Suzhou, China, pp. 267-271.

Wei, P., Cagle, L., Reza, T., Ball, J., and Gafford, J. (2018), LiDAR and camera detection fusion in a real-time industrial multi-sensor collision avoidance system. *Electronics*, Vol. 7, No. 6, pp. 1-32.